Nanofiber Self-Assembly

Deutsche Ausgabe: DOI: 10.1002/ange.201502177
Internationale Ausgabe: DOI: 10.1002/anie.201502177

SpONGE: Spontaneous Organization of Numerous-Layer Generation by Electrospray**

Gyuhyung Jin, Mikyung Shin, Seung-Hyun Kim, Haeshin Lee, and Jae-Hyung Jang**

Abstract: *Advanced technologies that can mimic hierarchical architectures found in nature can provide pivotal clues for elucidating numerous biological mechanisms. Herein, a novel technology, spontaneous organization of numerous-layer generation by electrospray (SpONGE), was developed to create self-assembled and multilayered fibrous structures. The simple inclusion of salts in a polymer solution prior to electrospraying was key to mediating the structural versatilities of the fibrous structures. The SpONGE matrix demonstrated great potential as a crucial building block capable of inducing sequential, localized drug delivery or orchestrating cellular distribution in vivo, thereby expanding its scope of use to cover a variety of biomedical applications.*

Layered structures are ubiquitous in nature. The macroscopic structure of skin, complete with the epidermis, dermis, and subcutaneous layers, is a representative example, and most organs such as the eye,[1] heart,[2] and blood vessels[3] in human possess a variety of functional layered structures. As observed in the outer membranes of microbes,[4] the cuticles of insects,[5] and the tough skin of plants,[6] layered structures generally exhibit multifunctionality. Layered structures are found not only in biological structures but also in consumer products. Examples include liquid crystal display panels[7] and solar cells.[8] The most distinct advantage offered by layered structures is that each layer possesses a different function that cooperates and interacts with the functions of adjacent layers.

To date, the range of techniques developed to fabricate multilayered structures is limited. Existing methods are able to build each layer manually one by one. The assembly of polyelectrolytes on solid substrates, referred to as layer-by-layer (LbL) deposition, has been widely implemented.[9] Multilayered microcapsules containing hydrophobic and hydrophilic drugs for drug delivery,[10] multifunctional layers loaded with vaccines,[11] enzymes, and catalysts[9] are examples of multilayered structures fabricated by LbL assembly. Spin coating is another method for producing multilayered structures. In particular, this technique has been used in semiconductor fabrication.[12] Recently, the preparation of hierarchical structures mimicking biological structures has involved the use of multilayer spin-coating methods followed by lithography.[13] Unlike the nonspontaneous processes developed by researchers, in nature, cells with distinct functions are spatially distributed and secrete various extracellular matrices (ECMs), which self-assemble to form multilayered structures spontaneously. Unlike the spontaneous formation of layered structures found in nature, man-made methods require the preparation of structures based on a repetitive process for each layer.

Herein, we demonstrate that electrospraying allows for the spontaneous formation of multilayered structures in a single, continuous spray of a polymer solution. The spontaneous formation of multilayers by an electrospray technique is an unconventional result considering that conventional electrospraying generates a nondiscrete, continuous fibrous structure. Techniques such as sequential electrospraying[14] or wet electrospinning followed by physical stacking[15] have previously been implemented to prepare structures mimicking blood vessels and other organs. However, the spontaneous formation of multilayered structures by a single, continuous electrospray of a polymeric solution has not been reported. We observed that the simple addition of organic/inorganic additives (sodium periodate, iron chloride, dopamine hydrochloride, and ethylamine hydrochloride) creates multilayered structures during the continuous electrospraying process. Due to the volumetric space between each layer, the thickness of the resulting sprayed structure was dramatically increased relative to that fabricated by conventional electrospraying (Figure 1 A). We named this technique spontaneous organization of numerous-layer generation by electrospray (SpONGE) because we obtained sponge-like multilayered matrices by a single electrospray process.

The notable volume expansion in SpONGE technique compared to that of conventional mats may be attributed to the increase in the electrical conductivity of salt–polymer

[*] G. Jin,[+] S. Kim, Prof. J. H. Jang
Department of Chemical and Biomolecular Engineering
Yonsei University
50 Yonsei-Ro, Seodaemun-Gu, Seoul, 120-749 (Korea)
E-mail: j-jang@yonsei.ac.kr
M. Shin,[+] Prof. H. Lee
The Graduate School of Nanoscience and Technology
Korea Advanced Institute of Science and Technology (KAIST)
291 Daehak-Ro, Yuseong-Gu, Daejeon, 305-701 (Korea)
E-mail: haeshin@kaist.ac.kr
Prof. H. Lee
Department of Chemistry
Korea Advanced Institute of Science and Technology (KAIST)
291 Daehak-Ro, Yuseong-Gu, Daejeon, 305-701 (Korea)
[+] These authors contributed equally to this work.

[**] This work was supported by the National Research Foundation of Korea (NRF) grant (2007-0056091 (J.-H.J.); Mid-career scientist grant, NRF-2014R1A2A1A01002855 (H.L.); Molecular-level Interface Research Center, SRC, 20090083525, (H.L.), Bio & Medical Technology Development Program (2013M3A9D3045879) funded by the Ministry of Science, ICT & Future Planning, and the Korea Health Technology R&D Project through the Korea Health Industry Development Institute, funded by the Ministry of Health & Welfare (HI14C1564).

Supporting information for this article is available on the WWW under http://dx.doi.org/10.1002/anie.201502177.

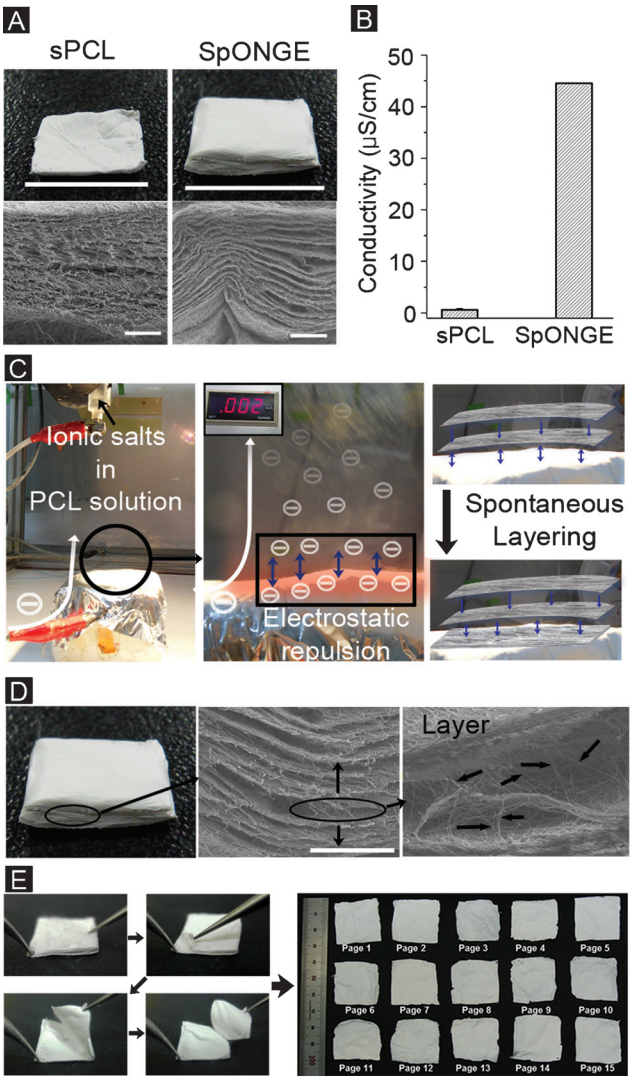

Figure 1. The generation of the SpONGE matrix. A) Digital and cross-sectional SEM images of sPCL and SpONGE, B) electrical conductivity of polymer solutions, C) schemes describing the proposed operational process for generating SpONGE matrices, D) the interspaces between each layer, and E) capability of the SpONGE to produce multiple uniform fibrous mats by manual manipulation. For detailed procedures, see the Movie 3. The scale bars represent 10 μm (digital image) and 100 μm (SEM).

mixtures (Figure 1B). The inclusion of organic/inorganic salts could result in a net increase in the electron density on SpONGE matrices, which could be explained by the noticeable electric currents (0.02 mA) measured between the ground collector and the nozzle (Figure 1C). No electric current is typically observed during conventional electrospraying, in which random scattering of fibers was observed. The remnant solvent can facilitate electron transfer for a net accumulation on the mats, ultimately producing electrostatic repulsion with newly formulated mats. Once the solvent is evaporated, the repulsive effects caused by electron accumulation can be dissipated, possibly formulating "sheet-like" mats at this moment. Subsequently, the continuous electrospray will generate another set of a net charge increase on the upcoming jets, possibly resulting in the formation of spontaneous layers and thin interspaces. Importantly, inter-networking adjacent layers through fiber branches in the interspaces (Figure 1D; arrows) are key features that are observed in SpONGE matrices, in contrast to conventional layered mats, which are composed of physically stacked layers. These fiber branches can play a crucial role in maintaining the structural integrity of SpONGE systems. The iteration of these dual effects (i.e., electrostatic repulsion and continuous electrospray) over several layers leads to the hallmark SpONGE effect.

Regardless of the types of polymers (polycaprolactone (PCL), poly(lactide-*co*-glycolide) (PLG), poly(vinylpyrrolidone) (PVP), and gelatin), SpONGE matrices were consistently observed to have formed once organic or inorganic salts were added to the polymer solutions prior to electrospraying (Figures S1 and S2). Thus, further studies were performed to fabricate multilayered PCL mats with dopamine hydrochloride, which were denoted SpONGE matrices. The thickness of the SpONGE matrices ranged from 502 ± 87.8 μm to 1695.3 ± 7.5 μm; thus, the matrices were approximately three- to six-fold thicker than conventional sheet-like PCL mats (sPCL), with the other processing parameters held constant (Figure S3). The differences observed during the electrospraying between SpONGE and the conventional process are visualized in Movies 1 and 2, respectively.

The SpONGE matrices could be split into multiple individual layers like a sheet of paper in a book by manually tearing them off (Figure 1E, see also Movie 3). The procedure used to prepare an individual layer is highly analogous to the manner in which strips of Scotch tape are pulled apart. The SpONGE matrices that were collected over 2 h generated over 15 thin fibrous mats by manual operation (Figure 1E). The ability to pull apart the fibrous layers manually was observed regardless of the polymer type used in any case in which organic or inorganic salts were incorporated (Figure S2).

The detailed characteristics of the SpONGE matrices and five split layers were compared with those of sPCL mats. No substantial alterations in the exterior fibrous morphologies were observed for any of the structures (Figure S4A). The presence of dopamine in the SpONGE matrices was confirmed by FTIR analysis, which detected characteristic peaks (815 cm^{-1}, 1504 cm^{-1}) corresponding to the phenyl ring in the catechol and amine groups (792 cm^{-1}; Figure S4B). Importantly, the inclusion of salts significantly modified both the surface and mechanical properties of the SpONGE matrices. Whereas the sPCL mats demonstrated typical hydrophobic properties ($125.6 \pm 4°$), the SpONGE matrices exhibited nearly zero hydrophobicity, as determined by static contact angle measurements, thereby potentially facilitating the rapid absorption of water-soluble biomolecules (Figure S4C). Both the SpONGE matrices and each individual layer demonstrated higher ultimate tensile strengths and shorter elongations at break than did the sPCL mats (Figure S4D). Interestingly, the SpONGE matrices exhibited stepwise fracture, which can be attributed to their multilayered structure. No significant differences in the Young's modulus among all conditions applied were observed. The enhanced

tensile strength of the SpONGE matrices may have resulted from the two-fold reduction in the fiber diameter (0.43 μm) relative to the fiber diameter of the sPCL mats (0.86 μm; Figure S4E).[15] This effect can be rationalized by the fact that more ordered crystal structures, which can reinforce the tensile strength, are normally observed in fibrous structures composed of thin fibers.[17] Notably, the separated individual layers exhibited nearly identical characteristics, indicating the homogeneity of each separated layer.

The SpONGE matrices demonstrated versatile capabilities to serve as controlled drug delivery vehicles. The hydrophilicity of the SpONGE matrices triggered the rapid absorption of immunoglobulin G and bovine serum albumin conjugated with a fluorescein isothiocyanate (IgG-FITC, BSA-FITC) throughout the entire multilayered structures (Figure 2A). However, complete wetting of the sPCL mats by the drug-containing solutions could not be achieved on the conventional sPCL mats due to its intrinsic hydrophobicity (Figure 2B). The drug-incorporation efficiency of the SpONGE matrices (97.59 ± 0.07 %) was significantly higher than that of the sPCL mats (20.56 ± 8.39 %). IgG-/BSA-FITC molecules were released from the SpONGE mats in a sustained manner without demonstrating any initial burst (Figure 2C). However, the majority of the IgG- or BSA-FITC molecules, which may have been mostly adsorbed onto the exterior of the sPCL mats, were released within one hour, after which no molecules were detected, presumably due to the shortage of drugs loaded into the sPCL mats. The sustained release of IgG- or BSA-FITC from the SpONGE matrices may have resulted from the existence of many interspaces, which could extend the drug path length or create reservoirs that could potentially delay the release of molecules from the matrices.

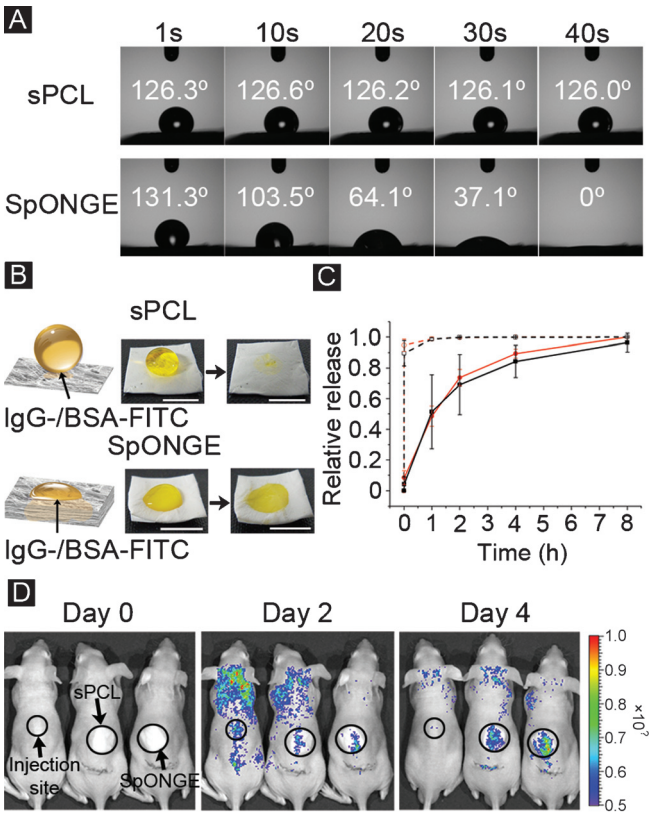

Figure 2. The ability of the SpONGE matrices to serve as drug carriers. A) Rapid wetting of the SpONGE matrices with water-soluble biomolecules, B) visualization of rapid and complete absorption of IgG-FITC molecules onto the SpONGE matrices, C) the relative released amounts of IgG-FITC (red dots) or BSA-FITC (black squares) released from sPCL (empty dots/squares) and SpONGE system (filled dots/squares) at different time points. D) Localized GFP expression at the implant site. Each matrix containing AAV-GFP vectors was subcutaneously implanted, and GFP-expressing cells were visualized using the Xenogen imaging system.

The immobilization of adeno-associated viral (AAV) vectors onto the SpONGE followed by its subcutaneous implantation onto the back of mice resulted in highly localized green fluorescent protein (GFP) expression at the implant site (Figure 2D). However, the bare adsorption of the majority of AAV vectors on the exterior surfaces of sPCL mats generated strong GFP signals in the distal region of the implanted sites. The many interspaces within the SpONGE matrices may have functioned as a reservoir block that could store gene vectors stably and possibly retard vector release toward the outer region. These structural effects of the SpONGE matrices may have allowed for the sustained release of gene vectors in vivo as well as localized gene expression adjacent to the implant site. Bolus AAV injection was accompanied by widespread GFP expression followed by its rapid termination, confirming the advantageous aspects of polymeric gene delivery for localized and extended gene expression.[18]

The SpONGE matrices demonstrated the ability to sequentially deliver dual drugs. The SpONGE matrices were partially separated into two parts, and two soluble model drugs, BSA-FITC and BSA-rhodamine (BSA-Rho), were dropped onto each partially peeled-off layer (Figure 3A). To characterize the release kinetics of two molecules, the SpONGE matrices containing two molecules in different layers were installed in a piston container, which could induce the unidirectional drug release (Figure 3B). Differences in drug path lengths as well as deviations in water penetration rates were key factors in modulating the sequential release of the two drugs (Figure 3C). Consequently, prior exposure of the BSA-FITC molecules in the upper part to an aqueous solution resulted in a faster release than that observed for BSA-Rho in the lower layer, possibly due to the shorter path length of BSA-FITC (Figure 3D). Due to their simplicity and capability of well separating multiple drugs, the SpONGE systems would be readily applied as platform vehicles for the spatiotemporal delivery of multiple biomolecules.

The subcutaneous implantation of the SpONGE matrices resulted in cellular alignment along the texture of the interspaces between fibrous layers, whereas infiltrating cells were randomly distributed across the sPCL mats (Figure 4). No toxicity of the SpONGE matrix to cells in vitro was confirmed prior to its implantation (Figure S5). Organizing cell populations is one of the critical issues in regenerative medicine because precisely mimicking cellular orientations and structural patterns can be highly pivotal in recovering the

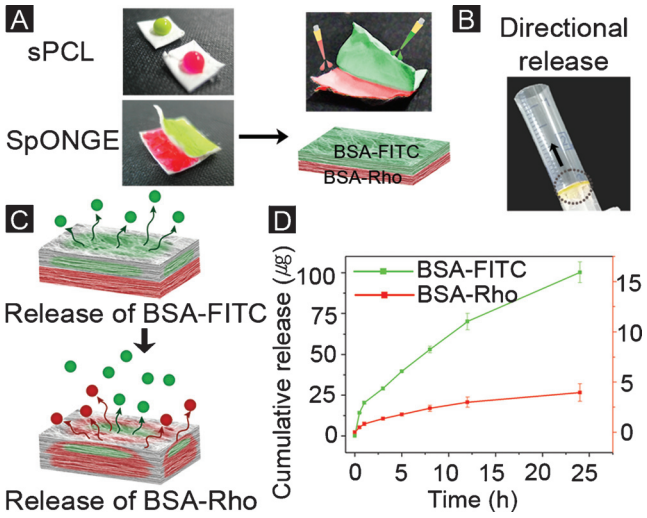

Figure 3. The sequential delivery of multiple drugs from the SpONGE matrix. A) The manner in which dual drugs can be loaded into the SpONGE matrices and B) a container capable of mediating unidirectional releases. C) Illustration demonstrating the differences in drug path lengths for their sequential delivery and D) the cumulative drug quantities released from the SpONGE matrices.

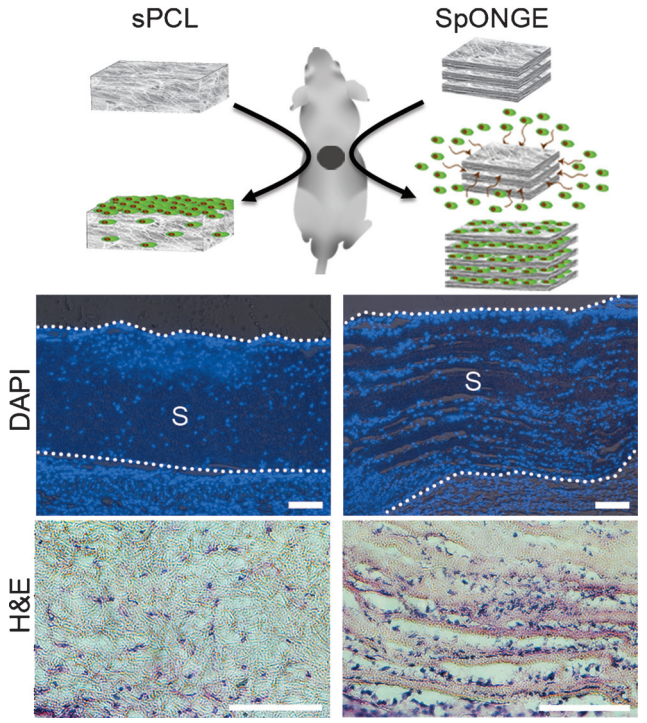

Figure 4. In vivo cellular distribution within sPCL and the SpONGE matrices subcutaneously implanted in mice. Cells infiltrated across the structures were stained using DAPI and H&E. "S" denotes the matrices implanted within mice. The scale bar represents 100 μm.

functionality of damaged organs.[19] Various approaches, such as bioprinting,[20] the use of patterned scaffolds,[21] and cell sheet technologies,[22] which typically require both complex equipment and specialized skills, have been employed to organize cellular distribution. Notably, the SpONGE system can induce cellular alignment in vivo without requiring additional sophisticated steps, indicating its great potential as an advanced platform capable of manipulating cellular orientations as well as patterns.

In conclusion, a novel SpONGE technology was developed for generating hierarchical multilayered fibrous systems by a single continuous electrospray. The incorporation of organic or inorganic salts in an electrospray solution is suitable for spontaneously forming multilayered fibrous structures. This process results in the volumetric expansion of the jetted materials, giving rise to a sponge-like structure. The SpONGE matrices demonstrated great potential as systems that can mediate the sequential delivery of multiple drugs, localized delivery, and the organization of cellular distribution. The application scope of the SpONGE system can be further extended to numerous fields that require control over biological events in a spatiotemporal manner, such as angiogenesis, cytokine signaling, and inflammation.

Keywords: electrospray · inorganic salts · multilayered nanofibers · organic salts · SpONGE

How to cite: *Angew. Chem. Int. Ed.* **2015**, *54*, 7587–7591
Angew. Chem. **2015**, *127*, 7697–7701

[1] F. Sommer, F. Brandl, A. Göpferich, *Adv. Exp. Med. Biol.* **2007**, *585*, 413–429.
[2] F. Torrent-Guasp, M. J. Kocica, A. F. Corno, M. Komeda, F. Carreras-Costa, A. Flotats, J. Cosin-Aguillar, H. Wen, *Eur. J. Cardio-thorac.* **2005**, *27*, 191–201.
[3] R. M. Nerem, D. Seliktar, *Annu. Rev. Biomed. Eng.* **2001**, *3*, 225–243.
[4] E. van Bloois, R. T. Winter, H. Kolmar, M. W. Fraaije, *Trends Biotechnol.* **2011**, *29*, 79–86.
[5] A. Ortiz-Urquiza, N. O. Keyhani, *Insects* **2013**, *4*, 357–374.
[6] A. Pauly, B. Pareyt, E. Fierens, J. A. Delcour, *Compr. Rev. Food Sci. Food Saf.* **2013**, *12*, 413–426.
[7] a) T. J. Scheffer, J. Nehring, *Appl. Phys. Lett.* **1984**, *45*, 1021–1023; b) B. M. Ocko, A. Braslau, P. S. Pershan, *Phys. Rev. Lett.* **1986**, *57*, 94–97.
[8] a) F. C. Krebs, J. Fyenbo, M. Jørgensen, *J. Mater. Chem.* **2010**, *20*, 8994–9001; b) I. O. Oladeji, L. Chow, *Thin Solid Films* **2005**, *474*, 77–83.
[9] K. Ariga, J. P. Hill, Q. Ji, *Phys. Chem. Chem. Phys.* **2007**, *9*, 2319–2340.
[10] U. Manna, S. Patil, *Langmuir* **2009**, *25*, 10515–10522.
[11] X. Su, B. Kim, S. R. Kim, P. T. Hammond, D. J. Irvine, *ACS Nano* **2009**, *3*, 3719–3729.
[12] J. J. van Franeker, D. Westhoff, M. Turbiez, M. M. Wienk, V. Schmidt, R. A. J. Janssen, *Adv. Funct. Mater.* **2015**, *25*, 855–863.
[13] H. Yao, H. Fang, X. Wang, S. Yu, *Chem. Soc. Rev.* **2011**, *40*, 3764–3785.
[14] a) H. Zhang, X. Jia, F. Han, J. Zhao, Y. Zhao, Y. Fan, X. Yuan, *Biomaterials* **2013**, *34*, 2202–2212; b) Q. P. Pham, U. Sharma, A. G. Mikos, *Biomacromolecules* **2006**, *7*, 2796–2805; c) S. Kidoaki, I. K. Kwon, T. Matsuda, *Biomaterials* **2005**, *26*, 37–46.
[15] R. Tzezana, E. Zussman, S. Levenberg, *Tissue Eng. Part C* **2008**, *14*, 281–288.
[16] J. S. Choi, S. W. Lee, L. Jeong, S. H. Bae, B. C. Min, J. H. Youk, W. H. Park, *Int. J. Biol. Macromol.* **2004**, *34*, 249–256.
[17] A. Baji, Y. W. Mai, S. C. Wong, *Mater. Sci. Eng. A* **2011**, *528*, 6565–6572.
[18] J. Jang, D. V. Schaffer, L. D. Shea, *Mol. Ther.* **2011**, *19*, 1407–1415.

[19] L. De Laporte, A. Huang, M. M. Ducommun, M. L. Zelivyanska, M. O. Aviles, A. F. Adler, L. D. Shea, *Acta Biomater.* **2010**, *6*, 2889 – 2897.
[20] S. V. Murphy, A. Atala, *Nat. Biotechnol.* **2014**, *32*, 773 – 785.
[21] S. Lee, S. Cho, M. Kim, G. Jin, U. Jeong, J.-H. Jang, *ACS Appl. Mater. Interfaces* **2014**, *6*, 1082 – 1091.
[22] K. Matsuura, R. Utoh, K. Nagase, T. Okano, *J. Controlled Release* **2014**, *190*, 228 – 239.

Received: March 8, 2015
Revised: April 3, 2015
Published online: May 8, 2015

